Research article

SURFACE and INTERFACE ANALYSIS

Received: 12 March 2012 Revised: 13 April 2012 Accepted: 13 April 2012 Published online in Wiley Online Library: 4 May 2012

(wileyonlinelibrary.com) DOI 10.1002/sia.5033

Simple universal curve for the energy-dependent electron attenuation length for all materials

M. P. Seah*

An analysis is presented for a simple, universal equation for the computation of attenuation lengths (*L*) for any material, necessary for quantifying layer thicknesses in Auger electron spectroscopy (AES) and X-ray photoelectron spectroscopy (XPS). Attenuation lengths for selected materials may be computed from the inelastic mean free path (λ_{Opt}) computed, in turn, from optical data. The computation of *L* involves the transport mean free path and gives good *L* values where values of λ_{Opt} are available. However, λ_{Opt} values are not available for all materials. Instead, λ may be calculated from the TPP-2M relation, but this requires the accurate estimation of a number of materials parameters that vary over a wide range. Although these procedures are all soundly based, they are impractical in many analytical situations. *L* is therefore simply reexpressed, here, in terms of the average *Z* of the layer which may be deduced from the AES or XPS analysis, the average atomic size *a* (varies in a small range) and the kinetic energy *E* of the emitted electron. For strongly bonded materials, such as oxides and alkali halides, a small extra term is included for the heat of formation. A new equation, S3, is established with a root mean square (RMS) deviation of 8% compared with the values of attenuation length calculated from λ_{Opt} available for elements, inorganic compounds, and organic compounds. This excellent result is suitable for practical analysis. In many films, an average value of *a* of 0.25 nm is appropriate, and then *L* may be expressed only in terms of the average *Z* and *E*. Then, *L* expressed in monolayers, equation S4, exhibits an RMS deviation of 9% for many elements. These results are valid for the energy range 100 to 30 000 eV and for angles of emission up to 65°. Copyright © 2012 Crown copyright.

Keywords: attenuation lengths; elements; IMFP; inelastic mean free path; inorganic materials; organic materials

Introduction

In the measurement of the thicknesses of thin films using X-ray photoelectron spectroscopy (XPS) or in principle Auger electron spectroscopy (AES), one of the most important parameters is the electron attenuation length, *L*. In using this as a parameter that is only dependent on the electron energy, *E*, and the material analysed, it is assumed that the intensity of, for instance, a substrate photoelectron line, I_0, is attenuated exponentially according to

$$I = I_0 \exp[-d/(L\cos\theta)] \quad (1)$$

where *d* is the layer thickness and θ is the angle of emission of the electrons from the surface normal. This approach is often referred to as the Beer–Lambert law or the straight-line approximation. It can give very precise and accurate results. For oxide thicknesses on an elemental substrate,[1] where the equations are reduced to

$$d = L\cos\theta \ln\left[1 + \left(R_{expt}/R_o\right)\right] \quad (2)$$

the direct relationship of *d* and *L* is very clear. In Eqn (2), R_{expt} is the measured ratio of the intensities for the oxide and elemental states from the layer and R_o is their ratio from the respective bulk phases. In more general cases, the equations are more complex,[2,3] but *d* and *L* are always directly related.

Right from the early days of XPS and AES studies, the attenuation length was recognised to be important. As a result of early measurements, three compilations of attenuation lengths were made,[4–6] culminating in very simple equations of the form:

$$L = kE^{0.5} + c \quad (3)$$

where *k* and *c* were listed constants, evaluated empirically. The experimental data showed large scatters that were later attributed to the likely effects of film non-uniformities. In 1982, Tougaard and Sigmund[7] showed that, even for ideal layers, as a result of the effects of elastic scattering, the decay of the substrate signal intensity with depth or film thickness was not quite the exponential used in the straight-line approximation of Eqn (1).

Extensive calculations of attenuation lengths are described by Jablonski and Powell.[8] Their calculations allow the intensities emitted in a given direction from a given depth to be determined. They defined a local effective attenuation length (EAL) that described the change in intensity with depth at a given depth to fit the straight-line approximation expression. They also defined a practical effective attenuation length (PEAL) that described the change in intensity between the surface and a given depth also to fit the straight-line approximation expression. This latter parameter matches the attenuation length, *L*, used by analysts to determine overlayer thicknesses. It is generally the case that *L* varies slightly with the layer thickness, *d*, such that *L* decreases over the first nanometre to an approximately constant value for angles of emission up to ~65° but, for higher angles, may rise significantly, particularly as the angle exceeds 70°. Jablonski and Powell[8] concluded that for an emission angle ≤65° and for layer thicknesses less than that which results in the substrate intensity

* Correspondence to: M. P. Seah, Analytical Science, National Physical Laboratory, Teddington, Middlesex TW11 0LW, UK. E-mail: martin.seah@npl.co.uk

Analytical Science, National Physical Laboratory, Teddington, Middlesex, TW11 0LW, UK

being reduced to 10% of its original value, the attenuation lengths are nearly constant and are useful for practical analysis.

In later work, Powell and Jablonski[9] reported EAL calculations involving elastic scattering via the Dirac–Hartree–Fock (DHF) potential rather than the Thomas–Fermi–Dirac (TFD) potential used earlier.[8] Jablonski, Salvat and Powell[10] showed that the differential scattering cross-sections calculated from the DHF potential agreed better with measured cross-sections. The newer EAL calculations for 16 photoelectron lines and 9 Auger electron lines from Si, Cu, Ag, W, Au, ZrO_2, $ZrSiO_4$, HfO_2 and $HfSiO_4$ generally exhibited changes from the EAL calculations using the TFD potential of less than 3% and were less than 1% in the great majority of cases.[9,11] More recent calculations for the ratio of L to the corresponding inelastic mean free path (IMFP), λ, have been made by Jablonski and Powell[12] who relate the ratio L/λ to the single scattering albedo, ω. These calculations, for the same 16 photoelectron lines and 9 Auger electron lines considered earlier,[9] averaged over many thicknesses and angles up to 50° gave the result

$$L/\lambda = 1 - 0.735\omega \tag{4}$$

Thus, if one knows ω and λ, L may be deduced. Values of λ may, for instance, be calculated using the relation TPP-2M,[13] whereas values of ω can be obtained directly from tables of coefficients for the elements[14] or from the transport mean free paths (TMFP), λ_{tr}. The TMFPs may be calculated from the elastic scattering cross-sections, σ, for the TFD potential using the table of coefficients given by Jablonski[15] or, for the DHF potential, using the table of Jablonski and Powell.[16] They may also be obtained from the NIST Elastic-Scattering Cross-Section Database (SRD64) versions 1.0 and 2.0 for the TFD potential and version 3.1[17] or later for the DHF potential. The relation between ω and λ_{tr} is

$$\omega = \frac{\lambda}{\lambda + \lambda_{tr}} \tag{5}$$

Thus, L is a useful parameter for angles of emission up to ~65°. Comparisons with experiments to test these predictions are very few because the manufacture of suitable samples is very demanding. Good agreement is found for SiO_2[18] and for organic materials[19] using, in each case, carefully prepared overlayer thicknesses. To circumvent the need to prepare layered materials, comparisons have been made for the IMFP via elastic peak electron spectroscopy, and, for elements, an agreement around 11% is found.[20] The value of the ratio L/λ is typically in the range 0.6 to 1.0, and so the contribution of further uncertainty from the errors in ω tends to be reduced.

For the analysis of arbitrary films, the situation is complicated because values of λ calculated from the optical data, λ_{Opt}, are only available for a limited number of materials.[13,21,22] For the IMFP, many analysts use the equation known as TPP-2M.[13] For TPP-2M, the user needs to know the number of valence electrons per molecule, N_v, the band gap for a non-conductor, E_g, the molecular mass, M, and the density, ρ, of the layer being analysed. In general, the layer may not be of an element or stoichiometric compound of known band gap. In the study of 41 elements by Tanuma, Powell and Penn,[21] N_v ranged over a factor of 11 and ρ over a factor of 42. The molecular weight is combined with N_v and ρ in the plasmon energy, E_p. In TPP-2M, λ is dependent on E_p^{-2}, and E_p^2 varied over a factor of 110 for the group of 41 elemental solids.[21] The response of λ to N_v, ρ and M is rather more complex than just the E_p component, and, for the 41 elemental solids at 1000 eV, a 10% error in each of these parameters results in root mean square (RMS) deviations for λ of 3.4%, 4.3% and 3.5%, respectively. With these changes in mind, it is difficult to see that the values of individual parameters for a general multielement film could each be estimated to the required 16% necessary for the overall uncertainty to be 10% or less.

For the mentioned reason, the simple relation of Cumpson and Seah,[23] called CS2, is often used for L. Cumpson and Seah's calculations are based on Hartree–Fock–Slater (HFS) potentials for the elastic scattering and are for thicknesses up to those that reduce the substrate intensity to 5% with angles of emission ≤58°. Their equation, for an element of atomic number, Z, with E in eV is

$$L = 0.316a^{3/2}\left\{\frac{E}{Z^{0.45}[\ln(E/27)+3]} + 4\right\} \text{ nm} \tag{6}$$

This relation was based on 27 elements and used the tabulated IMFP values of Tanuma, Powell and Penn.[24] The only required materials parameters are Z and a, and the atomic size deduced from the relation is

$$a^3 = \frac{10^{21}M}{\rho N_A(g+h)}\left(\text{nm}^3\right) \tag{7}$$

where ρ is the density in gm/cm^3, N_A is Avogadro's number, and g and h are the stoichiometries in the molecular formula G_gH_h of a molecule with molecular mass M. Of course, for the elements, $g = 1$ and $h = 0$.

The main advantage of Eqn (6) over the use of formulae for L/λ combined with computations of λ is that the only material parameters required are a and Z in which, for the study of 41 elements by Tanuma, Powell and Penn,[21] a only varies over a factor of 2.75. Indeed, for the mixtures of elements in general layers, the situation may be significantly better. An analysis of 87 oxides, 29 sulfides and 23 sulfates gives $a = 0.25 \pm 0.03$ nm, with a total range of a factor of only 1.75.[25]

Recently, a new equation was derived for λ that differs from TPP-2M in that N_v, E_g, M and ρ were eliminated and replaced by just a and Z with a small correction for the heat of reaction, H.[25] Of course, a is related to ρ and M through Eqn (7), but its range of variation is much smaller than either ρ or M. The new equation fitted the computations for elements,[21] inorganic materials[22] and organic compounds[13] to an RMS deviation of 8.4% if the IMFP computations from the optical data for the inorganic materials were corrected for the sum rule errors by a simple correction.[25] For the same basis, TPP-2M gives an RMS deviation of 12.0%. The new equation is thus much easier to use for complex layers and comes at no compromise to the accuracy. This equation for the IMFP in nm is

$$\lambda = \frac{(4 + 0.44Z^{0.5} + 0.104E^{0.872})a^{1.7}}{Z^{0.3}(1-W)} \text{ ″S1, IMFP in nm″} \tag{8}$$

where $W = 0.06H$ or $0.02E_g$ with H, the heat of reaction in eV/atom and both E and E_g the band gap in eV.

However, even combining Eqn (8) with computations of L/λ is not simple for the applied user, and so we consider the issue of calculating L more directly in the present article.

Establishing a simple relation for *L*

We seek a final relation for *L* like Eqn (8) if that is possible with reasonable accuracy. First, we generate *L* values from the computations of the IMFPs from the optical data, λ_{Opt}, for elements,[21] inorganic compounds[22] and organic compounds[13] by multiplying by the ratio L/λ as discussed earlier. Then, we describe *L* by a relation of the form of Eqn (8) and optimise the new coefficients by fitting. The numerical coefficients will mostly change from those in Eqn (8) because, for instance, L/λ has its own energy dependence that changes the power of *E* from 0.872, shown in Eqn (8), to a higher value. It is higher because L/λ is less than 1 at low energies and rises toward unity at very high energies.

Seah and Gilmore[26] analysed the attenuation length data of Cumpson and Seah[23] for the 396 photoelectric lines of Jablonski[27] to deduce a relation for L/λ involving both ω and *Z*. In that work, the elastic scattering cross-sections were from HFS potentials[23] and the ω values from TFD potentials.[14] The λ_{Opt} values were taken from Tanuma, Powell and Penn,[24] and the calculations were for electron emission at 45° to the surface normal. Here, we take the original 287 data values for 27 elements and 11 energies (energies at or above 100 eV)[23] to conduct a similar analysis as shown in Fig. 1. The least squares fit to these data, for $0.05 < \omega < 0.50$, is

$$L/\lambda = 0.975 - 0.6374\,\omega \qquad (9)$$

with a standard deviation of 0.017. The fit is better than previous one[26] because the data of Cumpson and Seah[23] are used directly instead of interpolating for the photoelectron lines used by Jablonski.[27] The *Z* term appearing in Eqn (35) of Seah and Gilmore[26] is now removed. This term may have arisen because, for the particular transitions then studied, the transition energies generally change with *Z*, adding a false correlation. That effect is removed in Eqn (9). Of course, for $\omega = 0$, $L/\lambda = 1$, Eqn (4) may appear more accurate, but the relation between L/λ and ω may involve higher powers of ω so that Eqn (9) is still valid in the range cited.

Jablonski and Powell[28] found, in their calculations for Si, Cu, Ag and W for a total of 13 transitions, that the slope on the plot for L/λ *versus* ω reduced slightly between the 0° and 45° emission. In their later work,[12] the same materials together with Au, ZrO_2, $ZrSiO_4$, HfO_2 and $HfSiO_4$ for a total of 25 transitions and averaged over the emission angles from 0° to 50° L/λ was as given in Eqn (4). Their data are entered in Fig. 1 as the crosses and can be seen to be within the scatter of the Cumpson and Seah data. Equation (9) fits Jablonski and Powell's data to an RMS deviation of 0.012. Equations (4) and (9) are very close, and so we shall continue by using both of these relations, although the figures are only plotted with Eqn (4) because those for Eqn (9) are not visibly different.

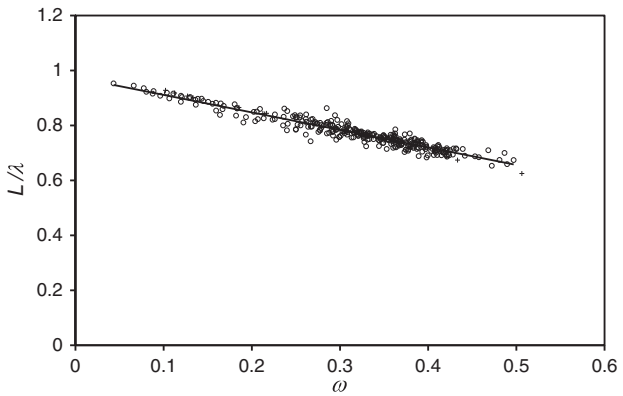

Figure 1. Ratio L/λ *versus* ω for (○) the data of Cumpson and Seah[23] for the HFS potential and for (+) Jablonski and Powell's data for the DHF potential[12] for $E \geq 100$ eV and for a layer thickness that reduces the substrate signal to 5%. The line is the least squares fit of Eqn (9).

We next need to calculate ω, and this is done as before[26] using the coefficients given by Jablonski and Powell[14] in their Table 1 or from Eqn (5) and the transport cross-sections of Jablonski[15] in his Table I for the TFD potential. For the DHF potential, we may use Table I of Jablonski and Powell[16] or SRD64.[17] For the TFD potential, in Jablonski and Powell's Table 1, values are calculated for 57 elements and the remainder (mostly gases or rare earth metals) being found by them by interpolation. This gives the result for ω as a function of *Z* shown in Fig. 19 of Seah and Gilmore.[26] For the DHF potential, accurate λ values are only available for the 41 elemental solids, and so ω values can only be calculated accurately for these elements from Eqn (5). Figure 2 shows the 41 values of ω as a function of *Z* for various energies using the DHF potential. Using the TDF and DHF potentials for ω, we may calculate L/λ directly from either Eqn (4) or (9) and hence, later, generate *L* values for the 41 elements[21] by four separate routes.

The calculations are a little more complex for compounds. For inorganic compounds, Jablonski and Powell[14] suggested evaluating an average atomic number $\bar{Z}$ from the stoichiometry

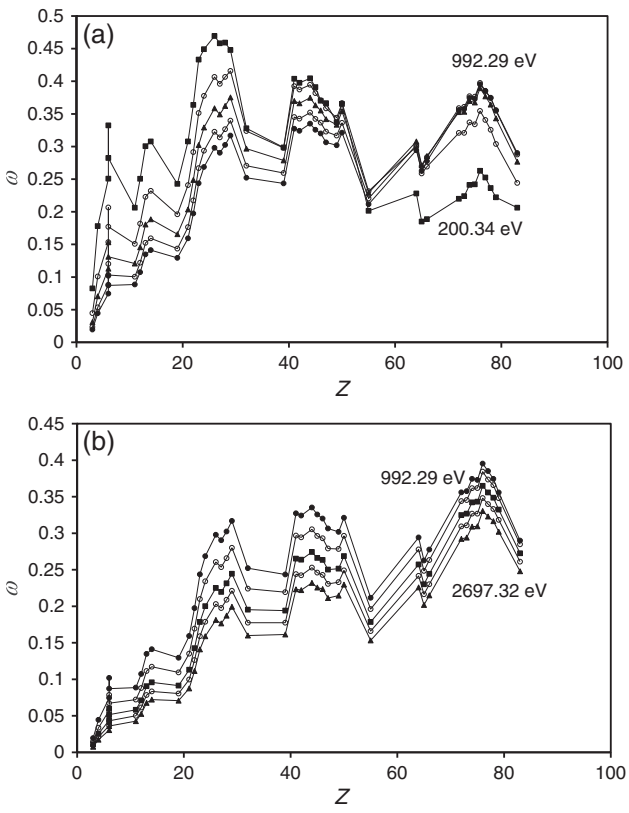

Figure 2. Values of ω for the various elements at (a) 200.34, 403.44, 601.86, 812.42 and 992.29 eV and (b) 992.29, 1339.45, 1808.07, 2208.38 and 2697.32 eV electron emission energy, using transport cross-sections for the DHF potential from SRD64[17] and the λ_{Opt} values of Tanuma, Powell and Penn.[21] The non-integer energy values derive from the data of Tanuma, Powell and Penn.[21]

of the material to calculate ω. However, we see from Fig. 19 of Seah and Gilmore[26] that, for example, a CuPd alloy at 1000 eV gives $\bar{Z} = 37.5$ with $\omega = 0.223$, whereas for Cu, $\omega = 0.307$, and for Pd, $\omega = 0.398$. A simple average of the ω values would be 0.353, significantly greater than 0.223 by using $\bar{Z}$, leading to L/λ = 0.750 instead of 0.833 – a difference of 10% in the final value of L. In more recent work, Powell and Jablonski[29] suggested a more accurate route by evaluating an average $\bar{\lambda}_{tr}$ via

$$\bar{\lambda}_{tr} = \left(N\sum_{i=1}^{m} x_i\sigma_i\right)^{-1} \quad (10)$$

where σ_i is the transport cross-section of the ith element and N is the compound atomic density. In the present work, we shall use Eqn (10) to deduce $\bar{\lambda}_{tr}$ from the σ_i values and hence ω from Eqn (5) with the IMFP given by calculated values of λ_{Opt}. Then, from Eqn (4) or (9), we obtain relevant values of L/λ, and again using λ_{Opt} we get values of L given the symbol L_{Opt} so that $L_{Opt} = (L/\lambda)\lambda_{Opt}$. These two routes give two slightly different values of L_{Opt} depending on the application of Eqn (4) or (9). As noted earlier, we use these two routes with both the DHF and TFD potentials in the present study to give the greatest robustness to the analysis. From the small changes seen by Powell and Jablonski,[9] we may expect similar final equations in each case.

The structure in the plots of ω *versus* Z may inevitably be thought to lead to increased uncertainty in our final expression for L. This issue may be clarified by proceeding directly to the plots of L/λ *versus* Z for the 41 elements of Tanuma, Powell and Penn[21] and many energies, a selection of which are shown in Fig. 3 and then returning to the compounds later. Figure 3 is

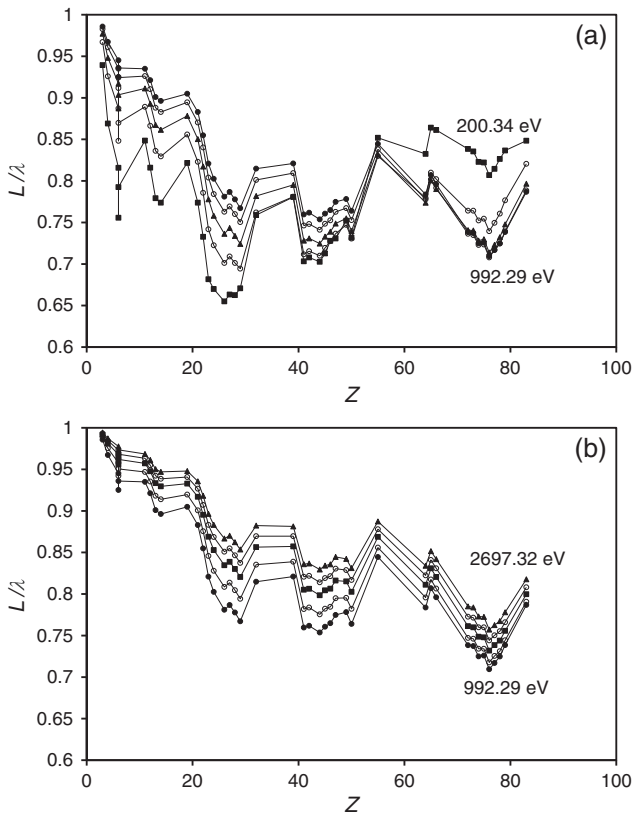

Figure 3. Values of L/λ for elements for (a) 200.34, 403.44, 601.86, 812.42 and 992.29 eV and (b) 992.29, 1339.45, 1808.07, 2208.38 and 2697.32 eV electron emission energy from Eqn (4) and Fig. 2.

calculated using Eqn (4), the ω values from the DHF potential[17] and the λ values from Tanuma, Powell and Penn.[21] We first try an equation of the form of Eqn (8) with new fitting coefficients except that for W which is unlikely to change. Of course, for the elements, $W = 0$. The result for L is

$$L = \frac{(5.8 + 0.0041Z^{1.7} + 0.088E^{0.93})a^{1.82}}{Z^{0.38}(1 - W)} \text{ ″S3, AL in nm″} \quad (11)$$

The small increases in the power of a and the overall power of Z are expected from their strong contributions to λ_{tr}.[15] Equation (11) describes the L data calculated from Eqn (4) and the λ_{Opt} data tabled by Tanuma *et al.*[21] for 41 elements in the energy range 100 to 30 000 eV to an RMS deviation of 8.0%. This compares remarkably well with the 8.5% found for Eqn (8) for the IMFPs. The RMS deviation here is calculated in the same manner as before[25] as the average of the RMS deviations for each of the 41 elements where, here, each of these deviations is determined at each of the 57 energies between 100 and 30 000 eV. These scatters are dominated by the between-element scatters at each energy, rather than the scatters over energy which have an average RMS deviation of 4.0%. Inspection of L_{S3}/L_{Opt}, where L_{S3} is from Eqn (11) and L_{Opt} is the value calculated from both Eqn (4) and the λ_{Opt} values tabled by Tanuma *et al.*,[21] shows no further a or Z dependence within the scatters that indicate that there are any further significant terms.

The RMS deviation given earlier is for the DHF potential and Eqn (4). It is useful to see how robust Eqn (11) is to the above four choices, and the RMS deviations for the computation using Eqn (9) or the TFD potential are given in Table 1. Using the earlier TFD potential leads to a small deterioration in the quality of the fit but not at a level that is significant, and changing from Eqn (4) to (9) has little effect.

Before moving on, it is worth evaluating the slightly simpler Eqn (6) from Cumpson and Seah.[23] There are now significantly more data available than were used in the original fitting. This equation gives an RMS deviation of 13.3% for the 41 elements, a useful value but significantly poorer than Eqn (11). If the powers of Z and a are changed to the optimal values in Eqn (11) and the other coefficients reoptimised, the RMS deviation would be improved.

Equation (11) shows that an excellent result may be obtained for L despite the strong changes of L/λ with Z seen in Fig. 3. The result for the distribution of the data about Eqn (11) is shown in Fig. 4 where the ordinate is $L_{Opt}Z^{0.38}/a^{1.82}$ and the single curve is $5.8 + 0.0041\ Z^{1.7} + 0.088E^{0.93}$ with Z set at 50. Of course, there should be a set of curves for different Z values, but they simply provide a small fan at low energies as shown in Fig. 6 of Seah.[25]

Table 1. RMS deviations for the data sets from Eqn (11) using different computational bases

	Eqn (4) and DHF potential	Eqn (9) and DHF potential	Eqn (4) and TFD potential	Eqn (9) and TFD potential
41 elemental solids	8.0	8.1	9.4	8.9
15 inorganic compounds	7.9	7.9	7.4	7.4
14 organic compounds	8.4	7.9	8.3	7.6
Overall, 70 materials	8.0	8.1	9.0	8.6

RMS, root mean square; DHF, Dirac–Hartree–Fock; TFD, Thomas–Fermi–Dirac.

SURFACE and INTERFACE ANALYSIS

The error bars shown represent the standard deviations of the ratios L_{S3}/L_{Opt} at each energy. Figure 4 does not change visually between the options of using the DHF or TFD potentials or using Eqn (4) or (9). Inspection of the residual contributions to the RMS deviations shows no remaining effects that could be attributed to a, Z, ρ or N_v. The sharp changes seen in Figs 2 and 3 from element to element and arising from the relative effects of λ_{Opt} and λ_{tr} are no longer evident, being subsumed into the residual 8% RMS deviation.

We may, perhaps, see why the sharp changes are removed by plotting (L/λ) values for $E = 544.58$ eV *versus* Z in Fig. 5 using Eqn (4). Here, (L/λ) values have simply been divided by $a^{0.21}$ with an extra scaling so that the ordinate is the same as that of Fig. 3. The points now scatter about a smooth curve with a standard deviation of 0.016 (note the offset zero), and much of the seemingly Z-dependent structure in Fig. 3 has been eliminated. This result indicates that much of the structure in Fig. 3 is atomic density related and that, to deduce (L/λ) for inorganic materials, we may use the value of a from Eqn (7) and the average $\bar{\lambda}_{tr}$ from Eqn (10). (L/λ) is now calculated with the values of λ_{Opt} for 15 inorganic compounds taken directly from Tanuma, Powell and Penn's[22] publication, which are then scaled for the effect of the f-sum and KK-sum scale errors as previously.[25] As before, Eqn (11) may be compared with the result using Eqn (4) and the elastic scattering via either the DHF or the TFD potentials. The RMS deviations are found to be an excellent 7.9% and 7.4%, respectively. The results for Eqn (11) and all four of the computational routes for L_{Opt} for the inorganic materials are given in Table 1. It is clear that differences are very small, and all agree very well with Eqn (11).

Figure 6 shows the plot like Fig. 4 for the inorganic compounds using Eqn (11) with the error bars calculated as for Fig. 4. The solid line is for $5.8 + 0.0041\ Z^{1.7} + 0.088E^{0.93}$ with Z set here at 26, same as the average of the 15 compounds studied. The RMS deviation calculated from the average RMS deviation for each compound over the energy range from 100 to 2000 eV is 7.9% or lower, as shown in Table 1. This is marginally better than the equivalent RMS deviation for the IMFPs.[25]

There are few accurate L values measured experimentally for inorganic materials, but recently, data for two energies have been obtained for thermal oxide layers.[18] These results are shown in Fig. 7 together with the plot for the attenuation lengths calculated from Eqn (11) and the PEAL values from the NIST program SRD82[30] using the input values for TPP-2M as listed by Tanuma *et al*.[24] The calculated values of L_{Opt} for SiO_2 based

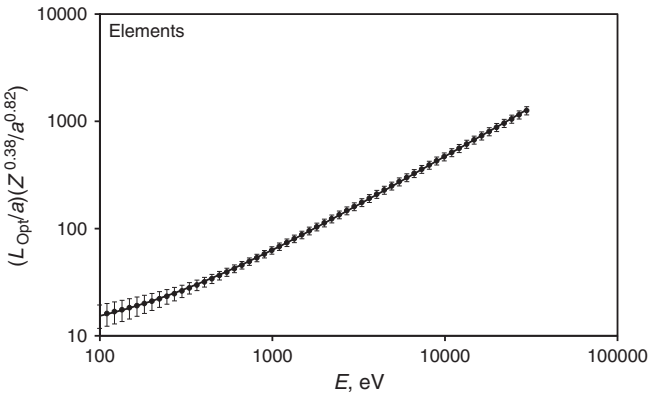

Figure 4. Plot of the average at each energy of $L_{Opt}Z^{0.38}/a^{1.82}$ *versus* E with associated error bars giving the RMS deviations from the function $5.8 + 0.0041Z^{1.7} + 0.088E^{0.93}$ for the 41 elemental materials of Tanuma, Powell and Penn.[21] The $a^{1.82}$ term has been split into two parts because L_{Opt}/a is the attenuation length in monolayers. The solid line shows the function $8.97 + 0.088E^{0.93}$ (i.e. near the middle of $5.8 + 0.0041Z^{1.7} + 0.088E^{0.93}$ with $Z = 50$). The RMS deviation is 8.0%.

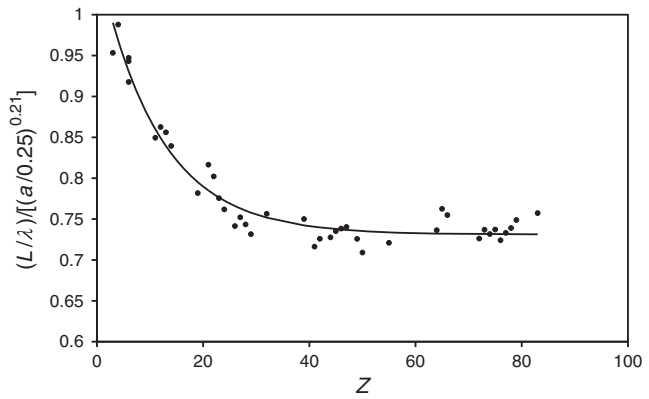

Figure 5. Plot of $(L/\lambda)(a/0.25)^{0.21}$ *versus* Z at 544.58 eV where the 0.25 has been included to bring the ordinate scale to the same range as in Fig. 3. (L/λ) is calculated from Eqn (4) for the 41 elemental materials of Tanuma, Powell and Penn.[21] The line is to guide the eye, but the scatter about this line is only 0.016 (i.e. 1.6%).

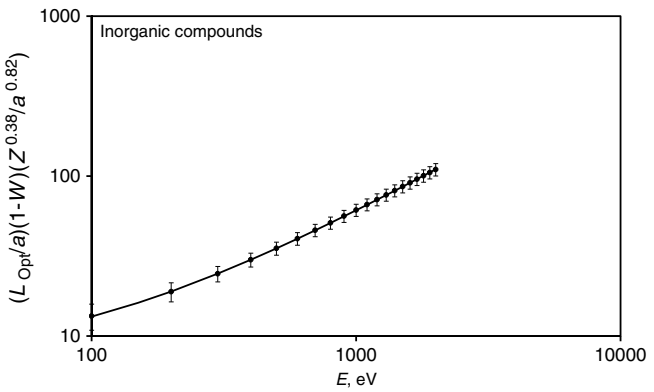

Figure 6. Same as in Fig. 4 but for the 15 inorganic compounds. The RMS deviation is 7.9%. The curve is as in Fig. 4 with $Z = 26$.

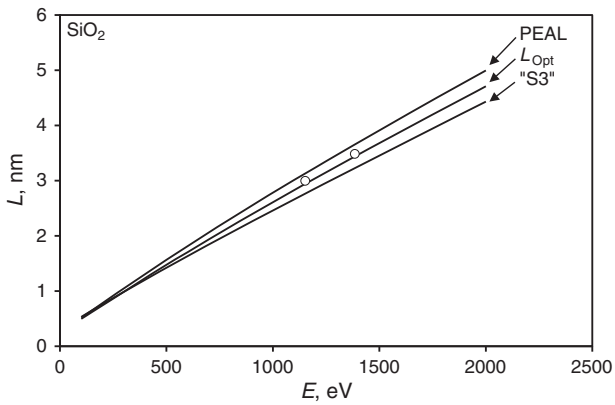

Figure 7. Results for SiO_2 using L_{Opt} calculated from λ_{Opt} corrected for the f-sum and the KK-sum rules[25] and using Eqn (4) and the DHF potential. Additional attenuation lengths are from S3 (Eqn (11)) and PEAL values from SRD82.[30] The two large solid circles are experimental data.[18]

on λ_{Opt} corrected for the f-sum and KK-sum rule errors[25] agree very closely with the measurements, and both the PEAL and Eqn (11) results diverge from L_{Opt} by less than 7%.

Finally, we should consider the organic materials. We first calculate L_{Opt} for each material from the λ_{Opt} values[13] with L_{Opt}/λ_{Opt} from Eqn (4) or (9). As before, the values of ω for each material are calculated from Eqns (5) and (10) and the transport cross-sections for both the TFD and DHF potentials. This gives directly the four sets of values of L_{Opt}. In evaluating Eqn (8) for the IMFPs,[25] it was found that the average Z and a values for all the organic materials could be taken as 4 and 0.25 nm, respectively. Using these values for all organics, we derive, from Eqn (11), one curve for L_{Opt} as a function of energy. Plotted as for the other materials, we then obtain Fig. 8 with an RMS deviation between Eqn (11) and L_{Opt} values of 8.4%. In an earlier study of L for organic materials over the energy range 500 to 1500 eV, it was found[19] by using the λ_{Opt} values that

$$L(E;\ \text{average organic}) = 0.00837E^{0.842}\ \text{nm} \qquad (12)$$

This is very close to the above result and exhibits an RMS deviation of 2.0% from Eqn (11) for the above energy range. It is plotted in Fig. 8 as the thin solid line joining the open square points at 500 and 2000 eV. The line is just visible, departing, as expected, at the lower energies. The lower power dependence of E (0.842) in Eqn (12) compensates for the other terms missing compared with Eqn (11).

Discussion

Thus, Eqn (11) provides a good overall correlation with L_{Opt} with an overall RMS deviation of 8.0% using Eqn (4) and 8.1% using Eqn (9) for all the materials sets. This is an excellent result and is comparable with the accuracy of the original computations for λ_{Opt}, estimated to be ~10%, on which this analysis is based.

The equivalent result using the earlier Eqn (6) for the elemental data is 13.3%, a good figure that could be reduced to 8.3% by refitting the six relevant coefficients.

Equation (11) allows L to be determined for complex films in which most materials parameters are unknown. If the average atomic size, a, is unknown, we found earlier that a value of

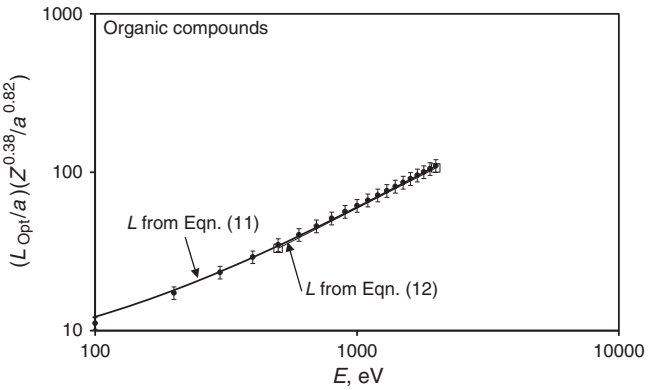

Figure 8. Same as for Fig. 4 but for the 14 organic compounds. The RMS deviation is 8.4%. Although Z and a are shown in the ordinate, the fixed values of $Z = 4$ and $a = 0.25$ nm have been used as discussed in the text. The curve is $5.843 + 0.088E^{0.94}$ (i.e. $5.8 + 0.0041Z^{1.7} + 0.088E^{0.93}$ with $Z = 4$). The earlier Eqn (12) is shown by the thin line joining the data points (□) at 500 and 2000 eV.

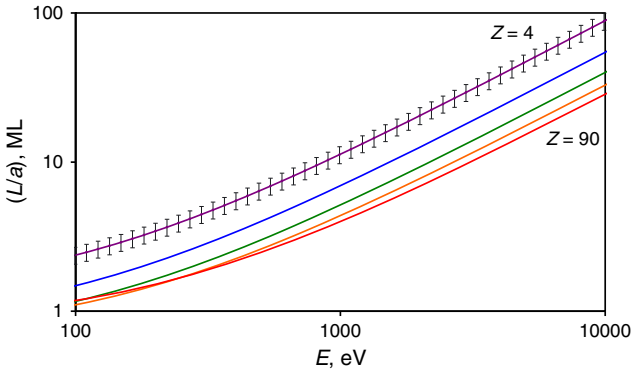

Figure 9. (colour online) Universal plot for L/a in monolayers (ML) for all materials using Eqn (13) with Z set at 4, 15, 35, 60 and 90 as in reference[25] with error bars of 12% shown only on the $Z = 4$ curve.

0.25 nm may be used.[25] The average a value for many elements and for 87 oxides, 29 sulfides and 23 sulfates was 0.25 ± 0.03 nm. If $a = 0.25$ nm is used for the computation of the elements, the RMS deviation is 22%, but for 34 elements excluding the large alkali metals, the small Be, graphite and diamond, it reduces to 15%.

When L is expressed in monolayers with $a = 0.25$ nm, as an analogue to equation S2 for the IMFP by Seah:[25]

$$L/a = \left(1.861 + 0.00132Z^{1.7} + 0.0282E^{0.93}\right)/Z^{0.38} \qquad (13)$$
$$\text{"S4, AL in ML, } Z \text{ dependence only"}$$

and the RMS deviation is 12%, as shown in Fig. 9. The RMS deviation falls further to 9% if the above seven elements are excluded. There is, of course, no need to exclude alkali metal compounds, as distinct from the metals themselves, because reaction reduces the volume generated by the important outer metal electron. The average alkali metal oxide has $a = 0.265$ nm, whereas the average alkali metal has $a = 0.40$ nm. For practical analysis, Eqn (13) is a very simple relation with excellent accuracy. The average Z value may easily be estimated from the analysis itself. Alternatively and even more simply, we may evaluate L removing the term in $Z^{1.7}$ and reoptimising to give L in nm as

$$L = \left(0.65 + 0.007E^{0.93}\right)/Z^{0.38}\ \text{nm} \qquad (14)$$
$$\text{"AL in nm, } Z \text{ dependence only"}$$

which has an RMS deviation of 18% for the 34 elements.

Conclusions

A simple universal curve for the attenuation length in nanometres or monolayers has been developed as the S3 equation, Eqn (11), which involves only the average atomic number and the average atomic size and, for inorganic compounds, the heat of formation. The dependence on this latter term is weak and is only significant for alkali halides and oxides. Equation (11) has an overall RMS deviation of 8% when compared with the calculated values for attenuation lengths. These were derived from the IMFPs from the optical data for elements,[21] inorganic compounds[22] and organic compounds,[13] with the data for inorganic compounds corrected[25] for the sum rule errors in the IMFPs. In addition, the L/λ values are calculated either using Eqn (4) or (9) with the transport cross-sections from either the DHF or TFD potentials. The individual RMS deviation values are given in Table 1 for these

SURFACE and INTERFACE ANALYSIS

four options for elements, inorganic materials and organic materials. The RMS deviations are all very consistent and support the use of the S3 equation, Eqn (11), for calculating the attenuation lengths necessary for determining layer thicknesses in AES or XPS. For situations where *a* is unknown, the S4 equation, Eqn (13), gives the attenuation lengths in monolayers only involving the average atomic number, *Z*, of the elements in the layer. This has an RMS deviation of 9% for 34 of the elements studied by Tanuma, Powell and Penn.[21]

Acknowledgements

The author thanks C.J. Powell for stimulating discussions. This work forms part of the Chemical and Biological Programme of the National Measurement System of the UK Department of Business, Innovation and Skills.

References

[1] M. P. Seah, S. J. Spencer, *Surf. Interface Anal.* **2002**, *33*, 640.
[2] P. J. Cumpson, *Surf. Interface Anal.* **2000**, *29*, 403.
[3] A. G. Shard, J. Wang, S. J. Spencer, *Surf. Interface Anal.* **2009**, *41*, 541.
[4] I. Lindau, W. E. Spicer, *J. Electron Spectrosc.* **1974**, *3*, 409.
[5] C. J. Powell, *Surf. Sci.* **1974**, *44*, 29.
[6] M. P. Seah, W. A. Dench, *Surf. Interface Anal.* **1979**, *1*, 2.
[7] S. Tougaard, P. Sigmund, *Phys. Rev. B* **1982**, *25*, 4452.
[8] A. Jablonski, C. J. Powell, *Surf. Sci. Rep.* **2002**, *47*, 33.
[9] C. J. Powell, A. Jablonski, *Surf. Interface Anal.* **2006**, *38*, 1348.
[10] A. Jablonski, F. Salvat, C. J. Powell, *J. Phys. Chem. Ref. Data* **2004**, *33*, 409.
[11] A. Jablonski, C. J. Powell, *Surf. Sci.* **2010**, *604*, 327.
[12] A. Jablonski, C. J. Powell, *J. Vac. Sci. Technol. A* **2009**, *27*, 253.
[13] S. Tanuma, C. J. Powell, D. R. Penn, *Surf. Interface Anal.* **1994**, *21*, 165.
[14] A. Jablonski, C. J. Powell, *J. Vac. Sci. Technol. A* **1997**, *15*, 2095.
[15] A. Jablonski, *Phys. Rev. B* **1998**, *58*, 16470.
[16] A. Jablonski, C. J. Powell, *Phys. Rev. B* **2007**, *76*, 085123.
[17] A. Jablonski, F. Salvat, C. J. Powell, NIST Electron Elastic-Scattering CrossSection Database, Version 3.1, SRD64, NIST, Gaithersberg MD, available at:http://www.nist.gov/srd/nist64.cfm
[18] M. P. Seah, S. J. Spencer, *Surf. Interface Anal.* **2005**, *37*, 731.
[19] M. P. Seah, S. J. Spencer, *Surf. Interface Anal.* **2011**, *43*, 744.
[20] S. Tanuma, T. Shiratori, T. Kimura, K. Goto, S. Ichimura, C. J. Powell, *Surf. Interface Anal.* **2005**, *37*, 833.
[21] S. Tanuma, C. J. Powell, D. R. Penn, *Surf. Interface Anal.* **2011**, *43*, 689.
[22] S. Tanuma, C. J. Powell, D. R. Penn, *Surf. Interface Anal.* **1991**, *17*, 927.
[23] P. J. Cumpson, M. P. Seah, *Surf. Interface Anal.* **1997**, *25*, 430.
[24] S. Tanuma, C. J. Powell, D. R. Penn, *Surf. Interface Anal.* **1991**, *17*, 911.
[25] M. P. Seah, *Surf. Interface Anal.* **2012**, *44*, 497.
[26] M. P. Seah, I. S. Gilmore, *Surf. Interface Anal.* **2001**, *31*, 835.
[27] A. Jablonski, *Surf. Interface Anal.* **1995**, *23*, 29.
[28] A. Jablonski, C. J. Powell, *Surf. Interface Anal.* **2002**, *33*, 211.
[29] C. J. Powell, A. Jablonski, *Nucl. Instrum. Meth. A* **2009**, *601*, 54.
[30] C. J. Powell, A. Jablonski, NIST Electron Effective Electron Attenuation Length Database, Version 1.1, SRD82, NIST, Gaithersberg MD, available at: http://www.nist.gov/srd/nist82.cfm

